1828
AKADÉMIAI KIADÓ

Data-driven lifetime estimation of solder joints with various geometries

Antal Bakonyi*, Zoltan Safar and Ambrus Miklos Zelei

Audi Hungaria Department of Whole Vehicle Engineering, Audi Hungaria Faculty of Vehicle Engineering, Széchenyi István University, Győr, Hungary

Received: December 31, 2024 • Revised manuscript received: June 12, 2025 • Accepted: June 18, 2025
Published online: October 1, 2025

Pollack Periodica • An International Journal for Engineering and Information Sciences

21 (2026) 2, 14–19

DOI:
10.1556/606.2025.01301

ORIGINAL RESEARCH PAPER

ABSTRACT

Virtual lifetime estimation of microelectronic devices has become essential, due to the tightening requirements and the trend of electronification. Thermal cycling load cause fatigue crack in solder joints and therefore functional failures. The application of the fatigue models viable in the literature is circumstantial for industrial scale problems. The exploitation of the already existing simulation data in data-driven models is a promising solution for speeding up the virtual lifetime estimation process. This paper benchmarks data-driven methods to predict the lifetime of solder joints with different geometric properties using a dataset originated from finite element simulation results. This case study shows that the nonlinear function fitting and the neural network are applicable.

KEYWORDS

lifetime estimation, fatigue, machine learning, solder joint, microelectronics reliability, artificial intelligence

1. INTRODUCTION

In microelectronics reliability, Machine Learning (ML) and Artificial Intelligence (AI) tools increasingly gain relevance. Engineering development processes and simulation tools rely on them more and more, since they can speed up the workflow by saving a lot of human effort. The electronics reliability is a specific area where ML tools come into the picture. The application of electronic systems is common in the field of general industry [1] and is also becoming increasingly relevant in the automotive industry [2]. In an electronic Printed Circuit Board (PCB), there might be hundreds or even thousands of electronic components. The weak point of the electronics assemblies are mostly the solder joints [3, 4]. Their analysis normally requires Finite Element (FE) analysis to predict the loads induced by vibrations or thermal stresses. The FE analysis requires pre-processing and post-processing, and these are the steps that involve huge amount of human effort. Especially, the diversity of the electronic components on a PCB - each type require a unique FE model. The rapid development of ML tools promises that this human effort could be one day completely replaced by computers. In the field of microelectronics reliability and lifetime prediction ML tools are gaining importance [5–7].

In several occasions, it is a problem that the origin of the train data is not completely consistent. For instance, lifetime data is coming from two different experiments, where the perfect match of circumstances could not be guaranteed. In this study, this effect is mimicked by obtaining the simulations by using a set of material models and the lifetime data were obtained from different lifetime models [8–10].

Industrial software tools [11] and on-line available packages [12, 13] provide many different options under the umbrella of the so-called machine learning tools. The deep understanding is not essential for engineers who apply these tools for problem solving. However, engineers must have well established experience when choosing from the large amount of ML tools.

*Corresponding author.
E-mail: bakonyi.antal@ga.sze.hu

AKJournals

As it is known in the literature by many researchers, the solder joint thermomechanic fatigue lifetime is affected by geometric parameters, like the standoff height of the Surface Mounted Device (SMD) [14, 15], the amount of solder volume in the solder joint connection [10, 15], the rate of angle offset of the SMD component from the nominal position [16, 17], and so on. It is relevant to note that in the case of standoff height, the higher value is better for thermomechanic lifetime, but it can be decreased the case of shock and vibration load [18].

The goal in this work to take simulation results from the classical FE approach. Then four methods will be benchmarked: the Inverse Distance Weighting (IDW) method, the Radial Basis Function (RBF) interpolation, the NonLinear Function Fitting (NLFF), and the Artificial Neural Network (ANN). The parameters of the benchmark test is which method gives the least Root Mean Square Error (RMSE) value predicting the lifetime and which method can be used for extrapolation.

2. METHODS

Simulation data were created by using FE simulations. Then four data-driven models were trained by a subset of the simulation data. Finally, their performance was compared by assessing the deviation from the test data set.

2.1. Simulation data

The simulation data are available in paper [10] in detail. The independent variables are the component standoff height h and the solder volume V underneath the component. The lifetime N is theoretically a function of the above independent variables. Simulations were conducted to obtain the data set of triplets of index $i = 1 \ldots n_X$: h_i, V_i, N_i. These data are put into vectors $\mathbf{h}$, $\mathbf{V}$, and $\mathbf{N}$. Three different material models are used for the simulation data: one elasto-plastic material model, Garofalo viscoplastic model and Anand viscoplastic model. For the test C0603m package type capacitor is modeled in Computer Aided Design (CAD) software and FE analysis is carried out from the results. From the 16 different lifetime predictions the averages of the estimated lifetimes are taken in account in the calculations.

2.2. Application of inverse distance weighting

Given the datapoints h_i, V_i and N_i, the approximating function N_{IDW} for the lifetime is obtained as

$$N_{IDW}(h,V) = \frac{\sum_i \frac{N_i}{(h_i-h)^2+(V_i-V)^2}}{\sum_i \frac{1}{(h_i-h)^2+(V_i-V)^2}} . \tag{1}$$

Equation (1) is a sum of functions. For each i-th function it is true that it gives N_i for any h_i, V_i and gives zero for any h_j, V_j; $i \neq j$ [19].

2.3. Application of radial basis function interpolation

The concept of the RBF interpolation is that the data is available in a grid-free form, i.e., the independent variables can have random distribution [20]. The basis function $\varphi(r)$ provides value 1 at the location of the input data and provides gradually decreasing value as the radius r increases measured from the input data location. The spread area of the individual basis functions is tuned by the value ε, with which

$$\varphi(r) = \frac{1}{\sqrt{1+(\varepsilon r)^2}} . \tag{2}$$

The approximating function of the lifetime $N_{RBF}(h,V)$ is composed as a sum of the basis functions:

$$N_{RBF}(h,V) = \sum_i \left(C_i \varphi\left(\sqrt{(h_i-h)^2+(V_i-V)^2} \right) \right) . \tag{3}$$

C_i is the i-th element of a vector of weights, obtained as

$$\mathbf{C} = \mathbf{A}^{\dagger}\mathbf{N}, \tag{4}$$

where $\mathbf{N}$ is the vector of existing lifetime data as defined in Section 2.1, $\mathbf{A}^{\dagger}$ represents the Moore-Penrose generalized inverse of matrix $\mathbf{A}$ [21], of which each element are obtained as:

$$A_{ij} = \varphi\left(\sqrt{(h_i-h_j)^2+(V_i-V_j)^2} \right) . \tag{5}$$

By using pseudo inverse it is allowed to have multiple lifetime values for a certain pair of standoff height and underneath volume portion.

2.4. Application of nonlinear function fitting

A continuous and differentiable function $N_{NLFF}(h,V,\mathbf{p})$ of the input parameters is assumed. Its derivative with respect to the parameters is $N_{NLFF,\mathbf{p}}(h,V,\mathbf{p})$. The goal is to find the parameters in vector $\mathbf{p} \in \mathbb{R}^{n_P}$ in such way that the sum $M(h,V,\mathbf{p})$ of the root square distance $e_i(h,V,\mathbf{p}) = N_i - N_{NLFF}(h,V,\mathbf{p})$ of the datapoints from $N_{NLFF}(h,V,\mathbf{p})$ is minimal [22]. The metric $M(h,V,\mathbf{p})$ is obtained as

$$M(h,V,\mathbf{p}) = \frac{1}{2}\sum_i \left(e_i^2(h,V,\mathbf{p}) \right) . \tag{6}$$

The following iteration minimizes $M(h,V,\mathbf{p})$:

$$\mathbf{p}^{k+1} = \mathbf{p}^{k} - L\frac{\partial M(h,V,\mathbf{p})}{\partial \mathbf{p}}, \tag{7}$$

where L is the learning rate and the derivative of the metric $M(h,V,\mathbf{p})$ is obtained as

$$\frac{\partial M(h,V,\mathbf{p})}{\partial \mathbf{p}} = -\sum_i \left(\frac{\partial N_{NLFF}(h,V,\mathbf{p})}{\partial \mathbf{p}} (N_i - N_{NLFF}(h,V,\mathbf{p})) \right) . \tag{8}$$

In the present study, the function, which is fitted to the lifetime data points is

$$N_{NLFF}(h, V, \mathbf{p}) = a_0 + a_1 h + a_2 V + a_3 h^2 \; . \qquad (9)$$

2.5. Application of artificial neural network

Programming the artificial neural network Scikit-learn python library and MLPRegressor function is used [12, 23]. MLPRegressor uses a Multi-Layer Perceptron (MLP) for regression tasks. Lifetime $N_{ANN}(h, V, \mathbf{p})$ is predicted after the neural network is trained with 3 hidden layers and 8, 4, 2 neurons in the layers.

2.6. Benchmark results evaluation

The RMSE is calculated for the IDW, RBF, NLFF and ANN models for different divisions of the train and test data. The average RMSE values were compared. IDW, RBF, NLFF and ANN used the same division of test and train data, when random division was applied. RMSE was calculated from the deviation between the test point and between fitted surface points after the training sequence.

In the first case group the test and train data is distributed by the geometry input method: EXT data results come from when geometry input method is a simple extrude command, REC and ELL data results are geometry input from loft command from rectangular and ellipse shapes, SE data results are from physics-based geometry inputs. In each case the volume and the lifetimes can vary, while the standoff height values are fixed at 3, 6, 9 μm [10]. In the second case group the data distribution is random. In the three case of randomly distributed test and train data the test points number is 3, and the train points number is 9, as in the first case group.

3. RESULTS

3.1. Benchmark analysis in the case of different division of test and train data

Figure 1 shows the IDW method fitting in the case where the simulation points from the EXT geometry input methods are the test points for the curve fitting. The surface is fitting without error on the training data-points. The fitted surface tracks the increasing lifetime trends in the vicinity of the test points, but extrapolating further, the trend of increasing lifetime does not maintained in the direction of increasing volume or standoff height.

Figure 2 shows the RBF method fitting in the case where the simulation points from the EXT geometry input methods are the test points for the curve fitting. The surface is fitting without error on the training data-points also in with this method. The fitted surface is only capturing the values in the close vicinity of the training data-points, otherwise the RBF method converge to zero.

Figure 3 shows the NLFF method fitting in the case where the simulation points from the EXT geometry input methods are the test points for the curve fitting. In this case

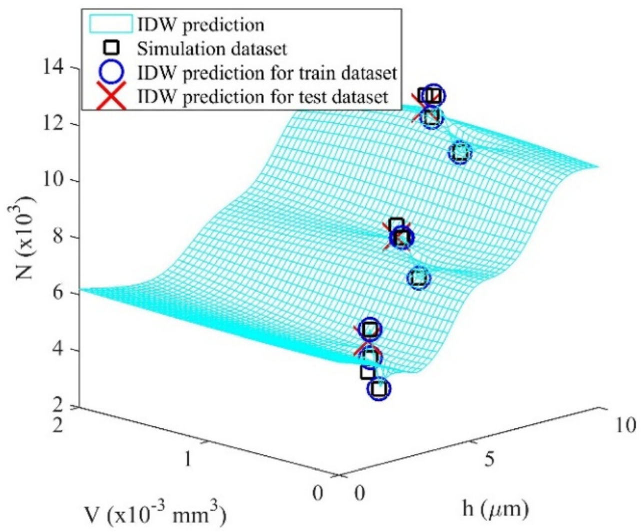

Fig. 1. Approximations with IDW method in the case of EXT division

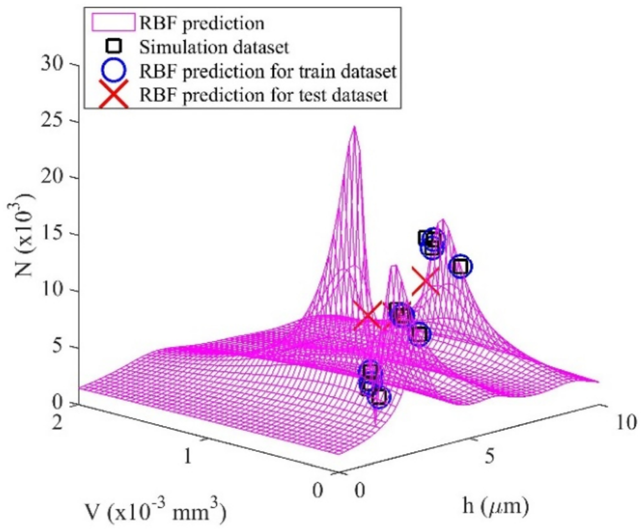

Fig. 2. Approximations with RBF method in the case of EXT division

the tendency of increasing lifetime is visible in both axes direction of increasing volume and increasing standoff height. The NLFF fitted surface is not fitting exactly on the training points.

Figure 4 shows the ANN-based fitting in the case where the simulation points from the EXT geometry input methods are the test points. The gradient of the fitted surface can change locally; in this case the fitted surface is tracking down the disturbances between the training data-points. The ANN fitted surface is also not fitting exactly on the training points.

In Fig. 5 the entire four fitted surface is plotted in the case of EXT division plotting further the fitted surfaces in both direction of the axes. The entire four fitted surface is accurate in the vicinity of the train points. However, in the case of extrapolation the prediction from the surface

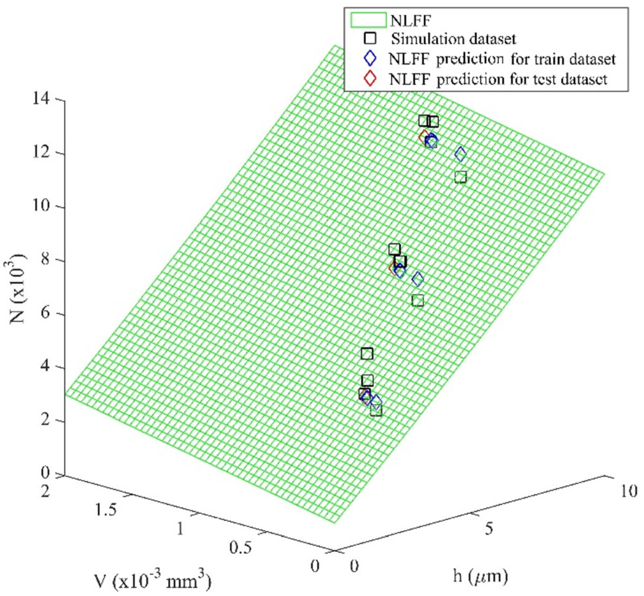

Fig. 3. Approximations with NLFF method in the case of EXT division

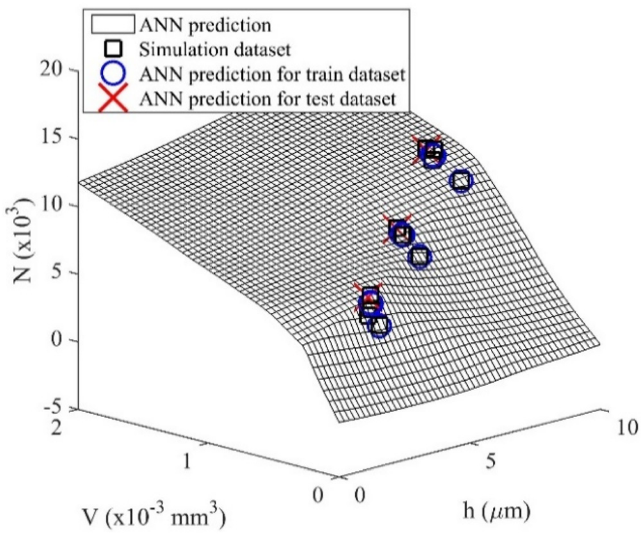

Fig. 4. Approximations with ANN in the case of EXT division

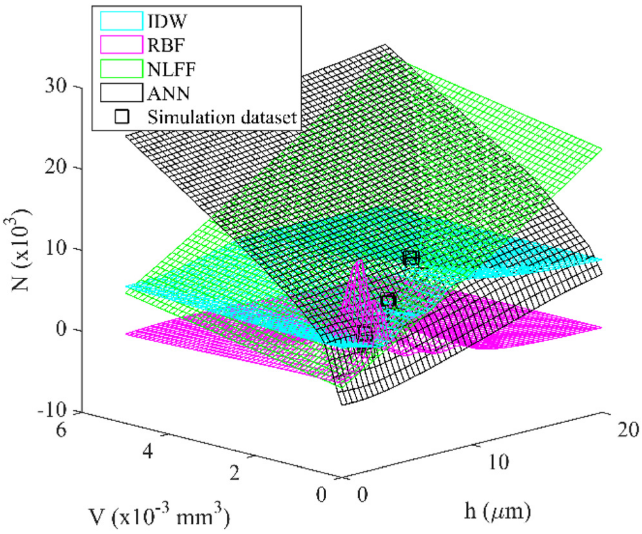

Fig. 5. Approximations with the four methods in the case of EXT division

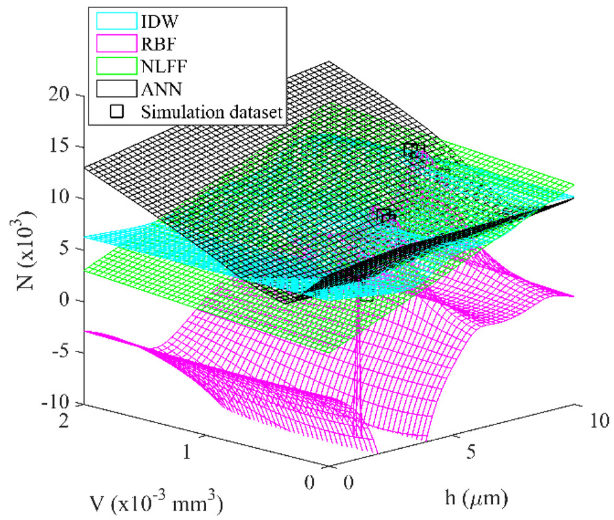

Fig. 6. Approximations with the four methods in the case 2 of random division

fitting methods can be very different. In the case of RBF method a prediction to a extrapolated point which standoff height and volume is high could be also converging to zero. In the case the NLFF and ANN is monotonically increasing in lifetime prediction with the increase of the volume or standoff height, while the IDW in the extrapolation area, over 9 μm starts to converge to a given value.

Figure 6 shows the case 2 of random division of the train and test data of the four surface fitting methods. In this case the RBF method predicts even negative lifetimes in the area of the lower standoff height values, while the fitted surfaces from NLFF, IDW, ANN methods are close to each others in the vicinity of the training datapoints.

4. DISCUSSION

In this chapter the quantitative and qualitative benchmark is presented of the four different methods. The RMSE values are compared in the case of different train and test data division introduced in the paragraph 3. The RMSE values are presented in Table 1 for every case, also the RMSE average values are written in the last row.

4.1. Benchmark analysis in the case of different division of test and train data

Figure 1 shows that the fitted surface with the IDW method track down the trained points without error and predicted lifetime is increasing monotonically in the function of the standoff height. However, the increase of the predicted

Table 1. RMSE values in the case of different test dataset

Test dataset	IDW	RBF	NLFF	ANN
EXT	0.72793	4.34510	0.54188	0.81390
REC	0.73656	0.85075	1.11350	0.88389
ELL	1.36320	26.7653	1.06360	0.68869
SE	0.69827	0.86984	0.46381	0.39360
Random case 1	0.77396	3.74410	0.22858	0.87570
Random case 2	0.86214	26.6907	0.37191	2.12970
Random case 3	1.17050	6.80450	0.45377	0.98287
RMSE AVG	0.90465	10.0100	0.60530	0.96691

lifetime is not captured in the direction of the volume, also in Fig. 5 it can be seen that the IDW predicted surface is not keeping the monotonically increasing lifetime tendency, so it is not applicable for extrapolating points which is not in the vicinity of the test points. It is also important to note, that in the case of interpolation the rate of change is not linear. The RMSE average value in Table 1 is the second least in the case of IDW method, but the application of this method requires caution.

In Fig. 2 the RBF method fitted surface can be seen, where the prediction could be much higher than the lifetimes from the training dataset, or lower, the predicted value can be even negative as in the case of Fig. 6. Overall the RBF method RMSE average value is the highest in Table 1, it is unstable and not applicable in this case of surface fitting.

The NLFF in Figs 3, 5, and 6 shows monotonic tendency for lifetime increase in both directions of the axes, and from this case study it gives the least RMSE average value in Table 1. However, the NLFF method requires prior knowledge of the training dataset to give the proper formula to the method. In this case the tendency of the training data-points fitting well on the given formula of NLFF.

ANN in Figs 4 and 5 shows good results from prediction, and the average RMSE value in Table 1 is close to the IDW RMSE average value. ANN can be applicable for interpolating points and for extrapolation as well, prior knowledge is not needed as in the case of NLFF method.

Overall in the case study the NLFF and ANN methods are good for lifetime prediction. The ANN is more flexible, while the NLFF method is more stable and gives less error in the prediction.

5. CONCLUSION

For extrapolation the ANN and NLFF methods are useful. IDW can be good for interpolation. RBF function is not applicable nor for interpolation nor for extrapolation in this case of train and test data division, because it predicts the lifetimes with small errors only in the close vicinity of the train points, otherwise the method converges to zero, or predicts negative lifetime. Comparing the results from the RMSE values, NLFF method gives the least prediction error to the test points overall, but it is important to note that previous knowledge is needed to use proper formula which can fit well on the dataset. IDW and ANN methods are also showed good predictions.

NLFF, IDW and ANN are also robust to the variation of the train and test dataset variations.

REFERENCES

[1] L. Ronai and T. Szabo, “Modeling and robotic handling of a snap-fitting box buckle,” *Pollack Period.*, vol. 15, no. 2, pp. 94–105, 2020.

[2] L. Porkolab and I. Lakatos, “Vehicle occupant safety development with finite element method,” *Pollack Period.*, vol. 16, no. 2, pp. 30–35, 2021.

[3] Q. Guo, M. Zhao, and H. Wang, “SMT solder joint’s semi-experimental fatigue model,” *Mech. Res. Commun.*, vol. 32, no. 3, pp. 351–358, 2005.

[4] J. A. Depiver, S. Mallik, and E. H. Amalu, “Thermal fatigue life of ball grid array (BGA) solder joints made from different alloy compositions,” *Eng. Fail. Anal.*, vol. 125, 2021, Art no. 105447.

[5] A. A. Salameh, H. Hosseinalibeiki, and S. Sajjadifar, “Application of deep neural network in fatigue lifetime estimation of solder joint in electronic devices under vibration loading,” *Welding in the World*, vol. 66, pp. 2029–2040, 2022.

[6] Y. Li, S. Askar, S. Paucar-Sullca, J. M. Burga-Falla, and R. R. Asaad, “A Bayesian neural network-based approach for multistate reliability assessment of solder joints exposed to various failure mechanisms,” *Vacuum*, vol. 222, 2024, Art no. 113004.

[7] M. Z. Akhtar, M. Schmid, A. Zippelius, and G. Elger, “Solder joint lifetime model using AI framework operating on FEA data,” *Eng. Fail. Anal., Part B*, vol. 167, 2025, Art no. 109032.

[8] S. Su, F. J. Akkara, R. Thaper, A. Alkhazali, M. Hamasha, and S. Hamasha, “A state-of-the-art review of fatigue life prediction models for solder joints,” *J. Electron. Packaging*, vol. 141, no. 4, 2019, Art no. 040802.

[9] W. W. Lee, L. T. Nguyen, and G. S. Selvaduray, “Solder joint fatigue models: review and applicability to chip scale packages,” *Microelectron. Reliability*, vol. 40, no. 2, pp. 231–244, 2000.

[10] A. Bakonyi, G. Fekete, and A. Zelei, “In silico benchmarking of fatigue life estimation models for passive SMD solder joints under thermal cycling,” *Appl. Mech.*, vol. 5, no. 4, pp. 877–907, 2024.

[11] Odyssee A-EYE, Hexagon, [Online]. Available: https://hexagon.com/products/odyssee?tabId=tab-690C6655F1D74C089356830F00306D55-2-1. Accessed: December 30, 2024.

[12] Scikit-learn, PyPI. [Online]. Available: https://pypi.org/project/scikit-learn/. Accessed: December 30, 2024.

[13] F. Pedregosa, G. Varoquaux, A. Gramfort, V. Michel, B. Thirion, O. Grisel, M. Blondel, P. Prettenhofer, R. Weiss, V. Dubourg, J. Vanderplas, A. Passos, D. Cournapeau, M. Brucher, M. Perrot, and É. Duchesnay, "Scikit-learn: Machine learning in Python," *J. Machine Learn. Res.*, vol. 12, no. 85, pp. 2825–2830, 2011.

[14] E. Suhir, S. Yi, J. Hwang, and R. Ghaffarian, "Elevated standoff heights of solder joint interconnections can result in appreciable stress and warpage relief," *J. Microelectron. Electron. Packaging*, vol. 16, pp. 13–20, 2019.

[15] J. Ha, Y. Lai, J. Yang, P. Yin, and S. Park, "Enhanced solder fatigue life of chip resistor by optimizing solder shape," *Microelectron. Reliability*, vol. 145, 2023, Art no. 114994.

[16] O. Krammer and Z. Illyefalvi-Vitéz, "Investigating the self-alignment of chip components during reflow soldering," *Period. Polytech. Electr. Eng.*, vol. 52, no. 1–2, pp. 67–75, 2008.

[17] J. Ha, K. Pan, H. Wang, D. H. Won, and S. B. Park, "The effect of misaligned passive component on fatigue life of solder joints and solder shape," in *2020 19th IEEE Intersociety Conference on Thermal and Thermomechanical Phenomena in Electronic Systems*, Orlando, FL, USA, July 21–23, 2020, pp. 1029–1034.

[18] S. Ghenam, A. El Hami, W. Gafsi, A. Akrout, and M. Haddar, "Optimal performance and cost-effective design of BGA solder joints using a deterministic design optimization (DDO) under real operating conditions," *Microelectron. Reliability*, vol. 146, 2023, Art no. 115019.

[19] J. Li and A. D. Heap, "A review of comparative studies of spatial interpolation methods in environmental sciences: Performance and impact factors," *Ecol. Inform.*, vol. 6, nos 3–4, pp. 228–241, 2011.

[20] R. L. Hardy, "Multiquadric equations of topography and other irregular surfaces," *J. Geophys. Res.*, vol. 76, no. 8, pp. 1905–1915, 1971.

[21] R. Penrose and J. A. Todd, "A generalized inverse for matrices," *Math. Proc. Cambridge Philosophical Soc.*, vol. 51, no. 3, pp. 406–413, 1955.

[22] S. L. Brunton and J. N. Kutz, *Data Driven Science & Engineering.* Cambridge: Cambridge University Press, 2019.

[23] F. Pedregosa, G. Varoquaux, A. Gramfort, V. Michel, B. Thirion, O. Grisel, M. Blondel, P. Prettenhofer, R. Weiss, V. Dubourg, J. Vanderplas, A. Passos, D. Cournapeau, M. Brucher, M. Perrot, and É. Duchesnay, "Scikit-learn: Machine learning in Python," *J. Machine Learn. Res.*, vol. 12, no. 85, pp. 2825–2830, 2011.